Semiconductor Optoelectronics
ISSN: 1001-5868

EVALUATION AND CLASSIFICATION OF COV-19 WITH ATTENTION BOTTLENECK RESIDUAL NETWORK

[1]Ahila T, [2]Dr.A.C. SubhaJini*

[1,2]Depantment of Computer Application, NICHE, Noorul Islam Center For Higher Education, Kumaracoil, India

e-mail: ahilaanishraj@gmail.com, * jinijeslin@gmail.com

ABSTRACT

Coronavirus disease (COVID-19), quickly distributing across the country, and earlier detection of COVID-19 was serious for providing effective healthcare to sufferers as well as protecting the uninfected population. As deep learning methods have shown potential in particular medical activities, they may be able to provide COVID-19 responses from medical photos of patients. The purpose of this research is to utilize DL with image processing to foretell who will contract COVID-19. The purpose of this research is to use X-ray photographs, ultrasound pictures, as well as CT scan photos to categorize COVID-19 sufferers as either abnormal or normal using the recently announced attention bottleneck residual network (AB-ResNet). It aims to separate the abnormally contaminated region from abnormal images using the recommended edge-based graph cut segmentation (E-GCS) method to locate the diseased area. The results examine how well the proposed method works in identifying COVID-19 with a high degree of accuracy (99%). We conclude that COVID-19 automatic identification may be improved with deep transfer learning as well as bottleneck feature extraction, resulting in better and more consistent overall performance.

Keywords: Attention bottleneck residual network; COVID-19 detection; deep learning; image processing, lung CT analysis.

INTRODUCTION

The World Health Organization (WHO) declared the SARS-CoV-2 virus-derived disease COVID-19 (COV-19) a global health emergency on March 11, 2020. More than 3 million individuals have lost their lives due to COVID-19, making it the ninth leading cause of death worldwide [1]. SARS-CoV-2 ribonucleic acid (RNA) in swab samples from the upper airways is detected using a polymerase chain reaction combined with reverse transcriptase (RT-PCR) [2]. Only people with evident illnesses are examined, and accurate findings take several hours to get [12], and many nations lack the resource's purpose of providing comprehensive testing. As a result, faster and more reliable screening procedures, such as imaging-based methods, are needed to complement or completely replace the PCR test. They may be employed in combination with RT-PCR to enhance diagnostic certainty or even instead of it in some places where RT-PCR is not commonly available[14]. In some circumstances, individuals by a

negative RT-PCR test have abnormal chest X-rays (CXRs), and Numerous reports have shown that CT scans of the chest are more sensitive for detecting COV-19 when RT-PCR is, suggesting suggested CT scans should be the primary method of investigation.

Several clinical analyses have found that the majority of COVID-19-infected individuals had lung infection symptoms [5]. Though RT-PCR, is a gold standard for recognition, CT shows a significant part in the finding and estimation of COVID-19's beneficial effect. The use of computer vision and DL techniques for an instinctive finding of various disorders and lesions, as well as the study of biomedical pictures, have yielded satisfactory outcomes in recent years [6,7]. DL-based findings and localization of COVID-19 on CT scans can give doctors quantitative auxiliary information. For CNNs to learn from scratch, they need a large number of labeled instances. In medical imaging applications like COVID-19 detection, were obtaining a larger amount of labeled CT scans is difficult, pre-trained CNNs skilled in a large variety of organic pictures could be used to extract features [8,9]. Each CNN's feature representation differs, as well as collective characteristics derived from several pre-trained CNNs, which can considerably improve finding capabilities. Even though computed tomography (CT) scans were more precise in finding lung disorders, chest X-ray pictures were still routinely employed [10,11]. This is mostly owing to the obtainability of a greater amount of X-ray devices, as well as the fact that it is less expensive and emits less radiation than CT scans.

X-ray pictures and DL models have recently been used in studies on the finding of COVID-19. Ozturk et al. [13], for example, developed a DarkCovidNet DL network that uses X-ray pictures to analyze COVID-19 automatically. The accuracy of the model was 87.02% for inter (COVID-19, ordinary, and pneumonia) as well as 98.08% for 2 (COV-19, normal) incidences. In its COVIDX-Net study, Hemdan et al. [4] made use of X-ray images. The COVIDX-Net model was trained using data from seven separate CNN experiments and tested on fifty X-ray photos for accuracy (25 normal and 25 COV-19 cases). Test accuracy was greatest for the three-class as well as binary-class CNNs in an investigation of CNNs with COVID-19 case classification conducted by Apostolopoulos et al. [3]. The ResNet50 model was used to achieve 98% testing accuracy according to Narin et al. [10] on a dataset of 100 images (50 normal and 50 COVID-19). Sethy and Behera [16] utilized thoracic X-ray pictures for feature extraction using a variety of pre-trained Cnn models. Compared to the Support Vector Machine (SVM) classifier, the ResNet50 classifier's 95.38% accuracy with 50 samples is the greatest (25 normal and 25 COV-19 cases). Social Mimic Optimization (SMO) was utilized to process the deep learning research characteristics, and then a support vector machine (SVM) was used on the combined functionality to generate effective features. For the COV-19 class and three additional cases, Farooq and Hafeez [4] developed a CNN model called COVID-ResNet based on ResNet (normal, microbial- and viral pneumonia). Using a freely available dataset, they were able to attain a 96.23 percent accuracy rate (COVIDx); nevertheless, only 68 COVID-19 specimens are used in our investigation. The most difficult aspect of using DL models is gathering a sufficient number of specimens with appropriate explanations for efficient training.

The research proposal for COVID-19 diagnosis followed an end-to-end framework that did not require any feature engineering development and could aid radiotherapists in many more reliably diagnosing COVID-19 infections. Therefore, the purpose of this work is to improve the accuracy of classifying COVID-19 patients into normal and pathological categories and

segmenting the aberrant area using deep learning. This approach is improved further by the fact that all three of the most important types of imaging techniques—ultrasound, computed tomography, and x-ray—are considered. We employed the COVID-19 chest imaging collection, pneumonia-, and normal chest pictures in this investigation. Before using deep learning models to train each picture, we standardized it.

PROPOSED METHODOLOGY

In a paper, researchers suggest DL-based techniques such as the attention bottleneck residual network (AB-ResNet) and edge-based graph cut segmentation (E-GCS). It's useful in several ways. It can increase the training pace of deep networks, decrease the number of parameters needed for a given network, and reduce the effect of the diminishing gradient problem, making it possible for connections to function well, especially in image analysis. These benefits motivate the current study's objective of using DL as well as image processing to categorize COVID patients as pathological or healthy. This detection is made using a series of methods. Figure 1 provides an overview of the entire procedure. Ultrasound images, CT scan images, and X-ray images are considered first. The visuals are then classified as abnormal or normal by using an attention bottleneck residual network (AB-ResNet) to analyze a single modality out of a set of potential ones. In this case, the ResNet is created by layering many attention components. Layer-specific features require modeling using a variety of attention masks. There may be an exponential demand for channels if we want to use a mask branch to get various factor permutations. Just after the abnormal class is categorized, edge-based graph cut segmentation (E-GCS) is used to automatically detect regions. Following this procedure aids in pinpointing the exact places where the sickness has spread. At last, we conduct a performance evaluation to see how well our system performs concerning the status quo.

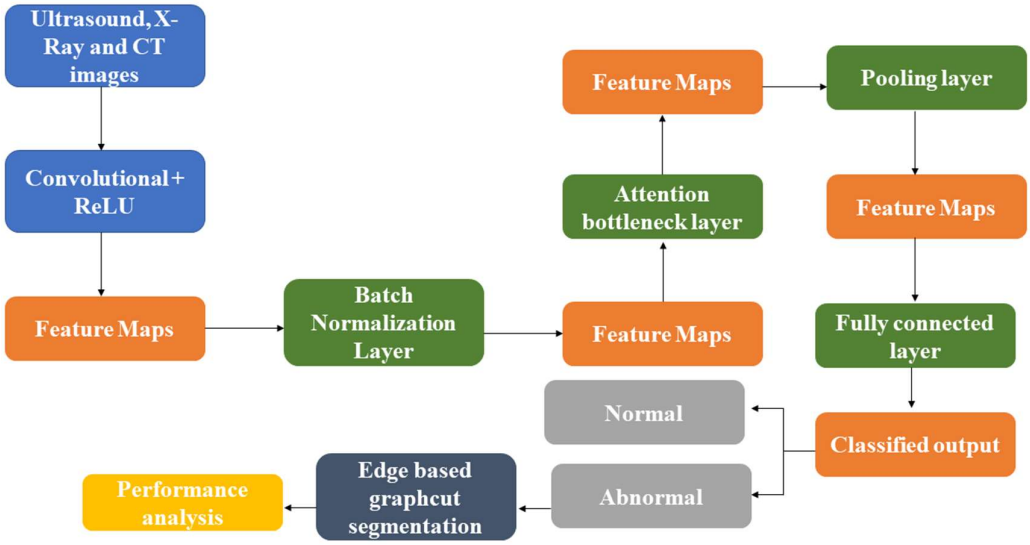

Figure.1. Overall view of the projected strategy for COV-19 testing

Figure 1 provides a schematic representation of the entire system that has been described. Additionally, an AB-ResNet block is made up of a GAP- (global average pooling), FC- (a fully connected) -layer, as well as two additional convolution layers. The COVID-19 set of data could've been denoted with the letters C, R, H, and W. Here, H, as well as W, stand for the dimensions of the height and width, respectively. The proposed AB-ResNet was trained with

input consisting of three-dimensional picture patches placed on label pixels to extract spatial-spectral properties. The location pixel indication is indicated by the picture patch label in this case. S S, representing the dimension of the feature of the neighborhood, is used to describe the size of an enhanced image. AB-main ResNet's variables, including the batch size, patch size, and learning rate, are set before the actual training begins. The suggested AB-ResNet is developed for 200 epochs, every of which is comprised of several mini-batch information and batch iterations. Each node in the network receives this as input. During model training, forward propagation is used to obtain the estimated label vectors for something like the training dataset. Then, the differences between the predicted label vectors and the corresponding label vectors transmitted by the GT tags are calculated using a CELF (Cross entropy loss function). In contrast to classifying ordinary and abnormal images, the suggested method uses objective functions to arrive at the final segmentation results, which aids in independently localizing the infected wound of the disease.

RESULTS AND DISCUSSION

The information gained after using the suggested method for determining the COVID & non-COVID situations has been explained in this chapter. A great amount of CT scans, ultrasound imaging as well as X-ray photographs were accessed from multiple publically available sources. With the development of COVID-19 remaining new, these enormous suppliers own much of any contextual information on COVID-19, hence necessitating the rely upon different datasets of non-COVID & COVID source photos. The accuracy is the proportions of successfully predicted pixels. It is expressed in equation (1) below. Overlapping value denotes the similarity measurements that reflect how the subdivision outcome of the principles equals the ground truth.

$$\text{Overlap} = TP/(TP + FP + FN) \quad \text{……..(1)}$$

where False positive, FP = incorrect found number as nodule pixels; true positive, TP = exactly found number as nodule pixels; True positive negative, TN = number of exact identification as background pixels. False Negative, FN= number of incorrect identification as background images. The values of calculation measures range from 0 to 1. The lesser FPR and FNR were good in subdivision performance. The performance evaluation is done by calculating the parameters of metrics like kappa and Jaccard coefficient, recall, F-score, NPV, accurateness, sensitive nature, specificity, exactness, Area under the curve (AUC), FPR, and FNR depicted in Table 1.

Table 1 demonstrates that the proposed system achieves a higher incidence of 0.9968 in terms of the overall comprehensive method when applied to the 3 imaging techniques. However, the rate of correctly classifying an X-ray image is determined to be 0.96, the probability of correctly categorizing a CT scan is 0.9328, as well as the rate of correctly categorizing an ultrasound imaging is 0.8665. Elevated concentrations of sensitivity, recollection, specificity, accuracy, kappa as well as Jaccard coefficients, and F-scores are all discovered. However, the anticipated scheme's lowest error rate in classifying images as abnormal or normal is shown to be an FNR rate of 0.0032.

Table 1. Performance analysis of the projected scheme

Performance metrics	Overall	X-Ray	CT	Ultrasound
Sensitivity	99.67	96.64	94.55	86.22
Specificity	99.66	95.42	92.25	86.95
Precision	99.67	95.36	92.05	87.08
Recall	99.671	96.64	94.55	86.22
NPV	0.997	0.9668	0.947	0.8609
FPR	0.003	0.0457	0.0774	0.1304
FNR	0.0032	0.0335	0.0544	0.1377
Accuracy	99.66	96.02	93.37	86.58
Kappa coefficient	0.9934	0.9205	0.8675	0.7317
AUC	99.67	96.03	93.04	86.59
Jaccard	0.9935	0.923	0.8742	0.7645
F-Score	0.9968	0.96	0.9328	0.8665

Therefore, the new system is more efficient than the current system, as shown by the performances and comparison study of the proposed scheme with 12 major performance indicators. As was previously indicated, the suggested approach takes into account CT scans, X-rays, & ultrasound pictures, all of which can be used to identify images as either normal or abnormal. While previous research has only taken CT scans into account, this new analysis incorporates data from all three major medical imaging techniques to demonstrate the test's efficacy in distinguishing between COVID-19 aberrant and normal patients.

Comparison with other Deep learning approaches

Five well-known pre-trained CNNs (VGG-16, VG-19, ResNet-18, ResNet-50, and ResNet-101) were employed to distinguish between COV-19 & non-COV-19 infections in this work. VGG-16 is a convolutional neural network (CNN) of 5 convolutional blocks (13 Conv layers) (fc6 to fc8). A layered tree, 5 convolutional blocks, 16 convolutional layers, and a total of 19 layers make up VGG-19 (fc6-8). The VGG-19 is superior to the VGG-16 due to its more complex CNN design, which consists of an extra layer. ResNet is an implementation of residual learning in a deep neural network. For training networks, this DL could make use of the layer data as a reference. ResNet-18, ResNet-50, and ResNet-101 each have their unique residual block. ResNet-18 is indeed a deep network consisting of 22 layers, the first of which is a convolutional layer. The network ends with such fully - connected layers. In every way, ResNet-50 is the same as ResNet-18, except that it uses a unique strategy for residual blocks and comprises a larger total number of residual blocks (16). Both ResNet-50 and ResNet-101 have 50 layers, while ResNet-101 has an additional 101 layers with 33 residual blocks. We used transfer learning to fine-tune the CNNs for such datasets. To solve this problem, a new input layer was added to the CNNs that was scaled to the scale of the contaminated areas (i.e., 60 x 60 x 1). The final, fully connected layer of such networks was also defined as a function

of the number of classes. Each network was trained with the same set of settings. Using an SGDM optimizer and a learning rate of 0.01 and a validation frequency of 5, we can get optimal results. The dataset was periodically created at each vintage, and if there wasn't any change between epochs, the procedure was stopped. Each network's training, as well as validation sets, made up 80% of the original dataset. All networks utilized identical validation and training sets to facilitate a direct comparison of their respective performances. All numerical methods were first tested for normality with the Kolmogorov-Smirnov procedure before statistical analysis. If the P-value is lower than 0.05, the hypothesis can be considered credible. Respectively. table 2 displays the results of an analysis of several different CNNs.

Table 2. Performance comparison of proposed with five CNN

Network	Group	Sensitivity (%)	Specificity (%)	Accuracy (%)
VGG-16	Training	80.63	86.76	83.70
	Validation	80.39	86.27	83.33
VGG-19	Training	94.85	79.41	87.13
	Validation	92.16	78.43	85.29
ResNet-18	Training	93.87	89.95	91.91
	Validation	95.10	88.23	91.67
ResNet-50	Training	96.50	100	98.28
	Validation	90.20	100	94.12
ResNet-101	Training	100	99.26	99.63
	Validation	100	99.02	99.51
AB-ResNet	Training	99.67	99.66	99.66
	Validation	99.52	99.58	99.57

The overall accuracy achieved was 99.57 %, which was higher than the performance of the other CNNs examined in this study. Because AB-ResNet uses just support vectors to build the separation hyperplane, an increase in the number of training samples does not affect accuracy.

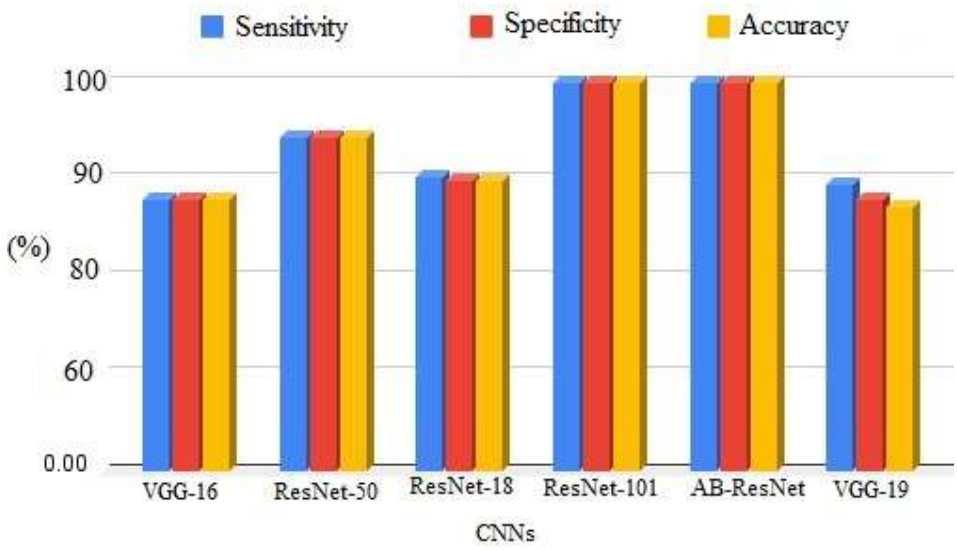

Figure 2. Performance evaluation with various CNNs

The study's drawbacks include the fact that the proposed system's performance was not compared to that of radiologists. The next step in this field of study will be to compare this technology to radiologists. Its most reliable method for confirming COVID-19 is RT-PCR. There are several drawbacks to this molecular assay, such as its high price, short supply, and need for well-equipped labs. Especially in low- and middle-income countries, these regulations can be a significant financial burden with uncertain benefits in terms of reducing disease transmission. Furthermore, monitoring and reducing the threat of COVID-19 requires operational and economic help in poor and intermediate countries due to inferior health systems.

In this research, we proposed using a convolutional neural network (CNN) trained on MRI, X-ray, and CT pictures to increase detection accuracy; this method applies to remote computer vision in any radiologist. As a result, the proposed system has the potential to alleviate radiologist workload and serve as a decision-support tool for COVID-19 infection.

CONCLUSION

Researchers in this study suggested using image recognition and DL to spot COVID-19. The aberrant and normal images were classified using an attention bottleneck residual network (AB-ResNet). By taking into account three distinct diagnostic imaging sense modalities (X-ray, CT, as well as ultrasound), the study also used edge-based graph cut segmentation (E-GCS) to sequence the disease contaminated area for localizing the illness. Important metrics such as accuracy, sensitivity, recollection, specificity, Area under the curve (AUC), kappa but also Jaccard coefficient, F-score, net present value (NPV), as well as false positive rate (FPR) are used to evaluate the proposed framework. The analytical results examined how well the suggested method detects abnormal and normal instances of COVID-19 with an amazing precision of 99.68% compared to the standard techniques. It can increase the network depth, leading to fewer variables, reduce the effect of the vanishing luminance problem, and help a network achieve high levels of accuracy in its image recognition quickly during training. Motivated by these merits, the current investigation seeks to use DL as well as image

processing to categorize COVID occurrences as abnormal or normal. This research may aid medical professionals in distinguishing between COVID and non-COVID cases, allowing for more precise disease localization.

REFERENCES

1. Abraham, B., & Nair, M. S. (2021). Computer-aided detection of COV-19 from CT scans using an ensemble of CNNs and KSVM classifier. *Signal, Image and Video Processing*, 1-8.
2. Angelov, P., & Soares, E. (2020). Towards explainable deep neural networks (xDNN). *Neural Networks*, *130*, 185-194.
3. Apostolopoulos, I. D., & Mpesiana, T. A. (2020). Covid-19: automatic detection from x-ray images utilizing transfer learning with convolutional neural networks. *Physical and Engineering Sciences in Medicine*, *43*(2), 635-640.
4. Farooq, M., & Hafeez, A. (2020). Covid-resnet: A deep learning framework for screening of covid19 from radiographs. *arXiv preprint arXiv:2003.14395*.
5. Hemdan, E. E. D., Shouman, M. A., & Karar, M. E. (2020). Covidx-net: A framework of deep learning classifiers to diagnose Cov-19 in x-ray images. *arXiv preprint arXiv:2003.11055*.
6. Kamal, K. C., Yin, Z., Wu, M., & Wu, Z. (2021). Evaluation of deep learning-based approaches for COV-19 classification based on chest X-ray images. *Signal, image and video processing*, 1-8.
7. Li, Y., Guo, K., Lu, Y., & Liu, L. (2021). Cropping and attention based approach for masked face recognition. *Applied Intelligence*, *51*(5), 3012-3025.
8. Ma, X., Zheng, B., Zhu, Y., Yu, F., Zhang, R., & Chen, B. (2021). COV-19 lesion discrimination and localization network based on multi-receptive field attention module on CT images. *Optik*, *241*, 167100.
9. Munusamy, H., Muthukumar, K. J., Gnanaprakasam, S., Shanmugakani, T. R., & Sekar, A. (2021). FractalCovNet architecture for COV-19 Chest X-ray image classification and CT-scan image Segmentation. *Biocybernetics and Biomedical Engineering*, *41*(3), 1025-1038.
10. Narin, A., Kaya, C., & Pamuk, Z. (2020). Automatic detection of coronavirus disease using X-ray images and deep convolutional neural networks. *arXiv preprint arXiv:2003.10849*.
11. Narin, A., Kaya, C., & Pamuk, Z. (2021). Automatic detection of coronavirus disease (covid-19) using x-ray images and deep convolutional neural networks. *Pattern Analysis and Applications*, 1-14.
12. Nayak, S. R., Nayak, D. R., Sinha, U., Arora, V., & Pachori, R. B. (2021). Application of deep learning techniques for detection of COV-19 cases using chest X-ray images: A comprehensive study. *Biomedical Signal Processing and Control*, *64*, 102365.
13. Ozturk, T., Talo, M., Yildirim, E. A., Baloglu, U. B., Yildirim, O., & Acharya, U. R. (2020). Automated detection of COV-19 cases using deep neural networks with X-ray images. *Computers in biology and medicine*, *121*, 103792.
14. Pahar, M., Klopper, M., Warren, R., & Niesler, T. (2021). COV-19 detection in cough, breath and speech using deep transfer learning and bottleneck features. *Computers in biology and medicine*, 105153.